



## Microbial diversity and antimicrobial susceptibility in endotracheal tube biofilms recovered from mechanically ventilated COVID-19 patients

Frits van Charante<sup>a</sup>, Anneleen Wieme<sup>b,e</sup>, Petra Rigole<sup>a</sup>, Evelien De Canck<sup>b</sup>, Lisa Ostyn<sup>a</sup>, Lucia Grassi<sup>a</sup>, Dieter Deforce<sup>c</sup>, Aurélie Crabbé<sup>a</sup>, Peter Vandamme<sup>b,e</sup>, Marie Joossens<sup>b</sup>, Filip Van Nieuwerburgh<sup>c</sup>, Pieter Depuydt<sup>d</sup>, Tom Coenye<sup>a,\*</sup>

<sup>a</sup> Laboratory of Pharmaceutical Microbiology, Ghent University, Ghent, Belgium

<sup>b</sup> Laboratory of Microbiology, Ghent University, Ghent, Belgium

<sup>c</sup> Laboratory of Pharmaceutical Biotechnology, Ghent University, Ghent, Belgium

<sup>d</sup> Department of Intensive Care, Ghent University Hospital, Ghent, Belgium

<sup>e</sup> BCCM/LMG Bacteria Collection, Laboratory of Microbiology, Ghent University, Ghent, Belgium

### A B S T R A C T

In patients with acute respiratory failure, mechanical ventilation through an endotracheal tube (ET) may be required to correct hypoxemia and hypercarbia. However, biofilm formation on these ETs is a risk factor for infections in intubated patients, as the ET can act as a reservoir of microorganisms that can cause infections in the lungs. As severely ill COVID-19 patients often need to be intubated, a better knowledge of the composition of ET biofilms in this population is important. In Spring 2020, during the first wave of the COVID-19 pandemic in Europe, 31 ETs were obtained from COVID-19 patients at Ghent University Hospital (Ghent, Belgium). Biofilms were collected from the ET and the biofilm composition was determined using culture-dependent (MALDI-TOF mass spectrometry and biochemical tests) and culture-independent (16S and ITS1 rRNA amplicon sequencing) approaches. In addition, antimicrobial resistance was assessed for isolates collected via the culture-dependent approach using disc diffusion for 11 antimicrobials commonly used to treat lower respiratory tract infections. The most common microorganisms identified by the culture-dependent approach were those typically found during lung infections and included both presumed commensal and potentially pathogenic microorganisms like *Staphylococcus epidermidis*, *Enterococcus faecalis*, *Pseudomonas aeruginosa* and *Candida albicans*. More unusual organisms, such as *Paracoccus yeei*, were also identified, but each only in a few patients. The culture-independent approach revealed a wide variety of microbes present in the ET biofilms and showed large variation in biofilm composition between patients. Some biofilms contained a diverse set of bacteria of which many are generally considered as non-pathogenic commensals, whereas others were dominated by a single or a few pathogens. Antimicrobial resistance was widespread in the isolates, e.g. 68% and 53% of all isolates tested were resistant against meropenem and gentamicin, respectively. Different isolates from the same species recovered from the same ET biofilm often showed differences in antibiotic susceptibility. Our data suggest that ET biofilms are a potential risk factor for secondary infections in intubated COVID-19 patients, as is the case in mechanically-ventilated non-COVID-19 patients.

### 1. Introduction

Since the start of the COVID-19 pandemic, respiratory coinfections have been reported in a large number of studies, and in the first small-scale studies during the initial outbreak in Wuhan (China), coinfections were reported in up to 50% of patients investigated [1]. There is however substantial variability in the reported prevalence of coinfections with some studies showing rates from 30% to 90% [2–5], whereas others report far lower rates [6–9]. Studies involving large patient cohorts show a percentage of clinically significant bacterial infections in hospitalized patients of around 4–14%, with the highest incidence being reported in patients on intensive care units (ICU) [10–12]. Although community acquired bacterial coinfections with

COVID-19 seems to be relatively uncommon, hospital acquired coinfections are reported more often (e.g., 47% of patients in eight Italian hospitals) [13,14]. A SARS-CoV-2 infection may lead to a compromised innate immune response at the infection site leading to an increased opportunity for bacterial attachment, growth, and dissemination [15]. Likewise, a bacterial infection might predispose to increased viral survival and replication, as host responses are affected, and coinfections may lead to more extensive tissue damage and a more excessive inflammatory immune response. In addition, extensive tissue damage likely facilitates further dissemination of the pathogens, thus increasing the risk of blood stream infections [15,16]. Complications from coinfections have also been noted in other respiratory diseases such as influenza where patients with coinfections have a significantly higher

\* Corresponding author.

E-mail address: [tom.coenye@ugent.be](mailto:tom.coenye@ugent.be) (T. Coenye).

<https://doi.org/10.1016/j.biofilm.2022.100079>

Received 20 February 2022; Received in revised form 2 June 2022; Accepted 2 June 2022

Available online 14 June 2022

2590-2075/© 2022 The Authors. Published by Elsevier B.V. This is an open access article under the CC BY-NC-ND license (<http://creativecommons.org/licenses/by-nc-nd/4.0/>).

mortality rate [17,18]. This has also been noted for COVID-19 when coinfections lead to further complications such as septic shock [13]. However, in a study with 142 patients who underwent bronchoscopy, untreated secondary respiratory infections were not associated with increased mortality, although the presence of specific bacteria (like the oral commensal *Mycoplasma salivarium*) could potentially be linked to a worse prognosis [19].

Mechanical ventilation via an endotracheal tube (ET) is used to support failing pulmonary gas exchange in critically-ill patients. Previous research has shown that biofilm formation on the ET has an impact on the incidence of bacterial infections in intubated patients and is a risk factor for the development of ventilator-associated pneumonia (VAP) [20,21]. A biofilm can form on the ET within 24 h of intubation and can act as a reservoir of microorganism that can subsequently cause infection in the lungs [22,23]. In addition, biofilm cells are intrinsically more tolerant to antibiotic treatment due to various factors (including lower metabolic rates of bacteria in the biofilm and poor penetration of antimicrobials into a biofilm), which can complicate the treatment of biofilm-related infections [24,25]. The hypothesis that biofilms on ETs play role in VAP is supported by the fact that in many cases the same bacteria are identified in ET biofilms and in other samples from the respiratory tract [26,27]. In addition, there is substantial evidence that modified ET releasing antimicrobial compounds can have a clinical impact by preventing biofilm formation [28]. For example, ET that release silver ions lead to a reduced adhesion of *P. aeruginosa* in an animal model and lower prevalence of VAP compared to uncoated tubes [29,30]. Other modifications, including coating with silicone or noble metals have also been described to reduce biofilm formation and could impact the development of VAP [31]. Such modified ETs could be used as such, or in combination with clearance devices [32].

In the present study, we investigated biofilms composition on 31 ETs recovered from intubated COVID-19 patients receiving care at Ghent University Hospital (Ghent, Belgium) during the first wave of the COVID-19 pandemic (Spring 2020), using culture-dependent and culture-independent methods, and determined the occurrence of antimicrobial resistance of the isolates recovered from these biofilms.

## 2. Materials and methods

### 2.1. Sample collection and processing

31 ETs were obtained from 31 mechanically ventilated COVID-19 patients admitted to the Intensive Care Units of Ghent University Hospital that were extubated between the 7th of April and 5<sup>th</sup> of May 2020. This study was approved by the Ethical Committee of Ghent University Hospital (registration number: B6702010156). Each ET (Fig. 1) was transversally cut open, the biofilm was scraped from the distal part of the ETs and subsequently resuspended in 500  $\mu$ L 0.9% (w/v) NaCl (physiological saline, PS). Subsequently, the ET was placed in a 50 mL falcon tube containing 10 mL PS, which was then vortexed and sonicated ( $3 \times 30$  s each). After removing the ET, the falcon tube was centrifuged at 5000 rpm (5804 R, Eppendorf, Hamburg, Germany) for 15 min, the supernatant was discarded, the pellet was resuspended in 1 mL PS, and combined with the earlier collected biofilm material. Half of this suspension was added to a Microbank vial which was stored at  $-80$  °C for subsequent culture-dependent identification. The other half was split in two, spun down at 5000 rpm (5804 R, Eppendorf) for 15 min, and after removing the supernatant, the pellets were frozen at  $-80$  °C until DNA extraction for culture-independent identification. Handling of samples potentially containing active SARS-CoV-2 was carried out in a biosafety

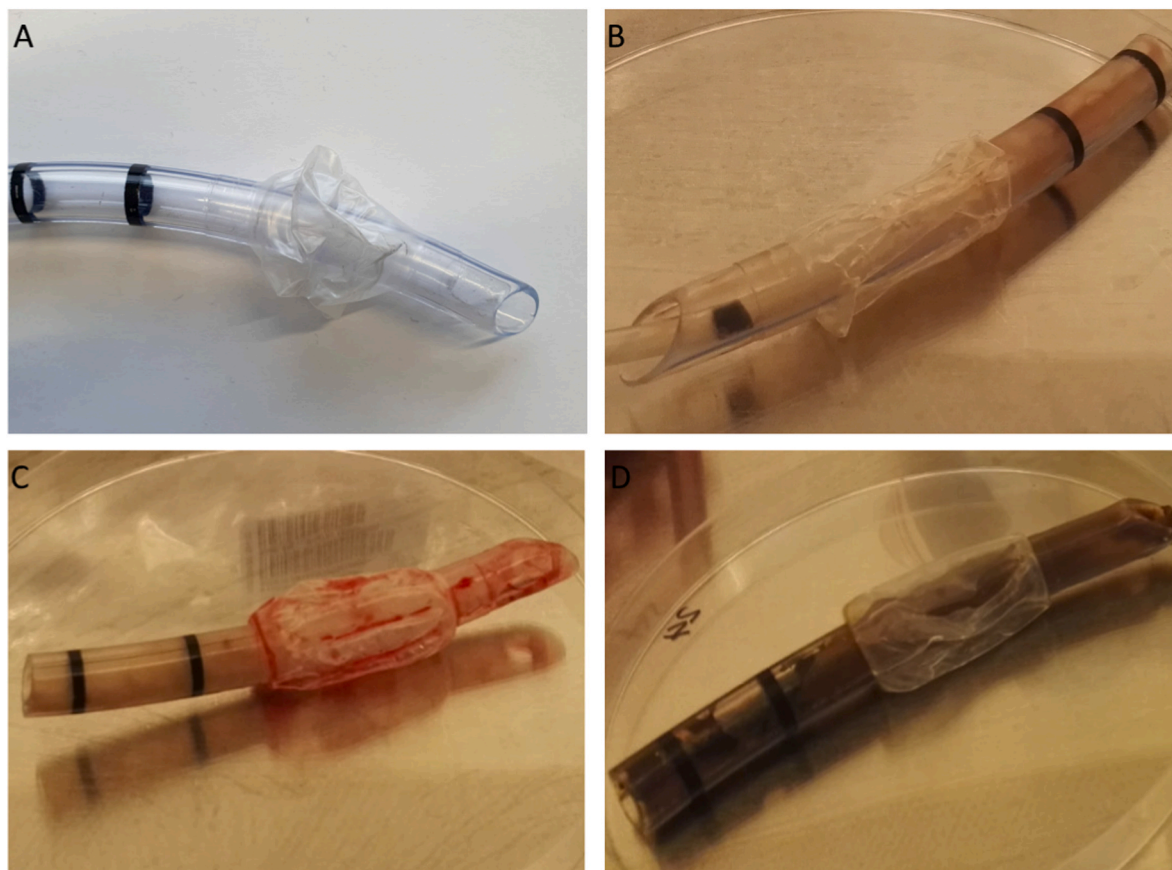


**Fig. 1.** A: Distal section of clean (unused) ET. B, C, D: Distal sections of ETs recovered from COVID-19 patients 17, 23, and 24 respectively prior to processing for biofilm recovery.

cabinet in a BSL-2 level facility (permit number AMV/121202/SBB219.2002/0916).

## 2.2. Plating and picking of colonies

From the Microbank vials stored at  $-80^{\circ}\text{C}$ , 10, 100, and 1000-fold dilutions were prepared in PS and plated under different oxygen conditions, i.e. aerobically, micro-aerobically at 3%  $\text{O}_2$ /5%  $\text{CO}_2$ /92%  $\text{N}_2$  in a BACTROX-2 Hypoxia chamber (SHEL LAB, Cornelius, USA) or anaerobically at 5%  $\text{H}_2$ /5%  $\text{CO}_2$ /90%  $\text{N}_2$  in a BACTRONEZ-2 anaerobic chamber (SHEL LAB). The following media and conditions were used: Mueller Hinton Agar (MHA) (Lab M Limited, Lancashire, UK) (aerobic and anaerobic incubation at  $37^{\circ}\text{C}$ ), Tryptone Soy Blood Agar (TSA blood agar) (Oxoid, Basingstoke, UK) (microaerobic and anaerobic incubation at  $37^{\circ}\text{C}$ ), TSA blood agar with 5  $\mu\text{g}/\text{mL}$  gentamicin (Oxoid) (microaerobic incubation at  $37^{\circ}\text{C}$ ), Mannitol Salt Agar (MSA) (Lab M Limited) (aerobic incubation at  $37^{\circ}\text{C}$ ), MacConkey agar (Lab M Limited) (aerobic incubation at  $37^{\circ}\text{C}$ ), Cetrimide agar (Lab M Limited) (aerobic incubation at  $42^{\circ}\text{C}$ ), Nutrient agar with 5  $\mu\text{g}/\text{mL}$  mupirocin and 10  $\mu\text{g}/\text{mL}$  colistin sulphate (NMC) (Lab M Limited; TCI Europe, Zwijndrecht, Belgium) (aerobic incubation at  $37^{\circ}\text{C}$ ) [33], Haemophilus isolation agar (Oxoid) (microaerobic incubation at  $37^{\circ}\text{C}$ ), Sabouraud agar (SAB) with 0.05 g/L chloramphenicol (Lab M Limited; Sigma-Aldrich, Saint Louis, USA) (aerobic incubation at  $37^{\circ}\text{C}$ ), Brain Heart Infusion agar with 5  $\mu\text{g}/\text{mL}$  vancomycin, 3  $\mu\text{g}/\text{mL}$  trimethoprim, 15  $\mu\text{g}/\text{mL}$  acetazolamide (BHIVTA) (Lab M Limited; Sigma-Aldrich) (aerobic incubation at  $37^{\circ}\text{C}$ ) [34], Acinetobacter CHROMagar (CHROMagar, Paris, France) (aerobic incubation at  $37^{\circ}\text{C}$ ), and VIA agar, consisting of 1 g/L beef extract (BD, Sparks, USA), 15 g/L peptone water (Oxoid), 10 g/L D-mannitol (Sigma-Aldrich), and 12 g/l agar (Lab M Limited) supplemented with 60 mg/L bromothymol blue, 5 mg/L vancomycin hydrochloride, 32 mg/L imipenem, and 2.5 mg/L amphotericin B (Sigma-Aldrich) (aerobic incubation at  $37^{\circ}\text{C}$ ) [35]. Morphologically distinct colonies were picked from plates incubated aerobically (after 24–48 h), microaerophilic (after 24–48 h) and anaerobically (after 48–72 h) and were subcultured on MHA, SAB, or TSA blood agar, until a pure culture was obtained. From these pure cultures  $-80^{\circ}\text{C}$  stocks in Microbank vials were prepared and stored.

## 2.3. Initial identification and dereplication

Isolates were subjected to basic microbiological tests and plated on selective media to allow recovery of as many different organisms as possible and to allow a first dereplication. The selective media used were the same as for the initial plating with the addition of Candida Colorex (bioTRADING Benelux, Mijdrecht, The Netherlands). Tests performed included the oxidase test (to check for cytochrome oxidase activity using tetra-methyl-p-phenylenediamine dihydrochloride), catalase test (to check for the presence of catalase activity using  $\text{H}_2\text{O}_2$ ), lysostaphin susceptibility (to differentiate *Staphylococcus* spp. from *Micrococcus* spp.), DNase activity (to check the production of DNase using an agar plate with DNA and precipitating with HCl), coagulase activity (to check for the production of coagulase using blood plasma), optochin susceptibility (to assist in identifying *Streptococcus pneumoniae*), bacitracin susceptibility (to assist in identifying *Streptococcus pyogenes*), and hemolysis (to differentiate isolates based on  $\alpha$ ,  $\beta$ , or  $\gamma$  hemolysis) [36,37].

## 2.4. Identification and dereplication using MALDI-TOF mass spectrometry (MS)

Isolates were subcultured twice on either MHA, SAB, or TSA blood agar. For the preparation of cell extracts, a 1  $\mu\text{L}$ -loopful of bacterial cells was suspended in 300  $\mu\text{L}$  of Milli-Q water and vortexed to obtain a homogeneous suspension. After adding 900  $\mu\text{L}$  of absolute ethanol, the suspension was mixed through inversion and centrifuged for 3 min at 14000 rpm at  $4^{\circ}\text{C}$ . Samples were stored at  $-20^{\circ}\text{C}$ . Prior to extraction,

samples were centrifuged as described above, supernatants were discarded and centrifugation was repeated to remove any residual ethanol, followed by air drying for 5 min at room temperature. The resulting pellet was suspended in 40  $\mu\text{L}$  of 70% formic acid and vortexed. Next, 40  $\mu\text{L}$  of acetonitrile was added and the mixture was vortexed. The extract was then centrifuged for 2 min at 14000 rpm at  $4^{\circ}\text{C}$  to remove cell debris and the supernatant, called the ‘cell extract’, was transferred to a new tube. Bacterial cell extracts (1  $\mu\text{L}$ ) were spotted in duplicate on a target plate (Bruker Daltonik, Germany) and air-dried at room temperature. The sample spot was overlaid with 1  $\mu\text{L}$  of matrix solution (10 mg/mL  $\alpha$ -cyano-4-hydroxycinnamic acid suspended in acetonitrile:Milli-Q water:trifluoroacetic acid [TFA] [50:47.5:2.5] solvent). Each target plate comprised one spot of pure matrix solution, used as a negative control, and one spot of Bacterial Test Standard (Bruker Daltonik, Germany), used for calibration. The target plate was measured automatically on a Bruker Microflex LT/SH Smart platform (Bruker Daltonik). The spectra were obtained in linear, positive ion mode using FlexControl software (version 3.4) according to the manufacturer’s recommended settings (Bruker Daltonik). Each final spectrum resulted from the sum of the spectra generated at random positions to a maximum of 240 shots per spectrum. Mass spectra generated were compared to the BDAL (MSP-8468, Bruker Daltonik) and the LM-UGent *in-house* (MSP-2876) identification databases and the identification log scores obtained were interpreted according to Bruker’s instructions. MALDI-TOF MS dereplication was performed using the SPeDE algorithm [38] in order to group isolates that represent the same taxon.

## 2.5. Culture-independent identification

DNA was extracted from cell pellets of the original samples as previously described [39]. In brief, cell pellets were resuspended in 400  $\mu\text{L}$  TE buffer (10 mM Tris, 1 mM EDTA, pH 8) to which 5  $\mu\text{L}$  of 0.5 M EDTA was added. The suspension was combined with 200 mg 0.1 mm silica: zirconia beads, 200 mg 1 mm silica:zirconia beads, and 1 chrome bead (Biospec Products, Bartlesville, USA) in a bead beat tube (Labconsult, Brussels, Belgium). Bead beating was done for 60 s using a bead mill homogenizer (Labconsult). Afterwards the tubes were incubated at  $95^{\circ}\text{C}$  for 5 min and cooled on ice. Lysozyme (Sigma-Aldrich) (final concentration: 3 mg/mL) and lysostaphin (Sigma-Aldrich) (final concentration: 0.14 mg/mL) were added, and tubes were incubated at  $37^{\circ}\text{C}$  on a shaker at 100 rpm for 60 min. Subsequently, proteinase K (ThermoFisher Scientific, Waltham, USA) was added (final concentration: 1.4 mg/mL), the tubes were incubated at  $56^{\circ}\text{C}$  for 30 min, and cooled on ice. 400  $\mu\text{L}$  of the cell lysate was transferred to a fresh tube. Subsequently, 180  $\mu\text{L}$   $\text{dH}_2\text{O}$  was added to the original tube and again transferred to the fresh tube to minimize DNA loss. Subsequently, 400  $\mu\text{L}$  of 5 M NaCl and 1 mL phenol:chloroform:isopropylalcohol 25:24:1 (Sigma-Aldrich), were added, mixed, and incubated at room temperature for 20 min while shaking at 100 rpm. Then, the tubes were spun down at 13000 g for 20 min, the top 800  $\mu\text{L}$  of the aqueous layer was transferred to a fresh tube, and combined with 106  $\mu\text{L}$  7.5 M ammonium acetate and 906  $\mu\text{L}$  ethanol. After precipitation on ice for 30 min, the supernatant was removed and the DNA was cleaned up using QIAEX II Gel Extraction Kit (Qiagen, Hilden, Germany). After DNA extraction, library generation and sequencing was performed according to the Illumina protocols for 16S rRNA gene and ribosomal internal transcribed spacer 1 (ITS1) sequencing [40,41]. Sequences were analyzed using the DADA2 pipeline [42] after primer removal using the Cutadapt tool [43], which was all performed in R. Taxonomy was assigned by using the SILVA version 132 database [44] for the 16S rRNA sequencing data and the UNITE version 8.3 database [45] for the ITS1 data. Alpha diversity was calculated using the phyloseq R package [46]. Analysis of correlation between diversity indexes and sequence abundance was done using SPSS Version 26 (SPSS Inc., Chicago, USA). Sequencing data has been deposited in the EMBL-EBI database under accession number PRJEB47052.

## 2.6. Antimicrobial susceptibility testing

Antimicrobial susceptibility towards a selection of antibiotics commonly used to treat lower respiratory tract infections was determined using disc diffusion according to the European Committee on Antimicrobial Susceptibility Testing (EUCAST) guidelines [47] using MHA for all isolates, except for *Streptococcus* and *Candida* spp. isolates for which it was performed on TSA blood agar [47] and MHA supplemented with 2% glucose [48], respectively. The following antibiotic discs were used: aztreonam 30 µg (AZT), ceftazidime 30 µg (CAZ), clindamycin 2 µg (CDM), gentamicin 10 µg (GEN), meropenem 10 µg (MEM), moxifloxacin 5 µg (MXF), and vancomycin 30 µg (VAN) (Oxoid). For the *Candida* spp. isolates the following discs were used: caspofungin (CAS) 5 µg, fluconazole (FLU) 25 µg, itraconazole (ITR) 50 µg, and nystatin 100 µg (Labconsult). The zone of inhibition was measured after 18 h of incubation. MICs of fluconazole and itraconazole were determined for *Candida albicans*, *Candida tropicalis*, and *Candida parapsilosis* isolates according to the EUCAST guidelines [49]. Antimicrobial resistance was classified based on EUCAST breakpoints except for caspofungin where CLSI breakpoints were used (due to a lack of breakpoints in the EUCAST guidelines). Isolates were classified as: susceptible (S) (high likelihood of therapeutic success), intermediate (I) (high likelihood of therapeutic success with increased dosage), or resistant (R) (high likelihood of therapeutic failure) [50–52].

## 3. Results and discussion

### 3.1. Culture-dependent identification

In total, 832 isolates from 31 patients with COVID-19 were recovered. After dereplication, 430 isolates were selected for analysis by MALDI-TOF MS. This approach allowed to cluster and identify the isolates, and 2 to 11 MALDI-TOF MS clusters (a cluster being defined as a set of isolates representing the same mass spectrometry-defined independent strain [38] were identified per patient (Supplementary Table S1). In samples from 20/31 patients 6 or less clusters were identified. The most commonly identified species were *Staphylococcus epidermidis* (recovered from 24/31 patients), *Candida albicans* (22/31 patients), *Enterococcus faecalis* (10/31 patients), *Pseudomonas aeruginosa* (8/31 patients), and *Klebsiella aerogenes* (8/31 patients) (Table 1). While MALDI-TOF MS did not allow identification of all isolates at the species level (for 216/430 isolates MALDI-TOF MS only allowed identification to the genus level), in some cases species-level identification was still possible based on the already performed initial basic microbiological tests, e.g. for *Candida* spp. isolates and these are included in Table 1.

Among the isolates we identified commensal as well as potentially pathogenic bacteria. This included common presumed commensals such as lactobacilli and *Prevotella* spp., but also more unusual species such as *Slackia exigua*, an anaerobic Gram-positive member of the human oral microbiota that is occasionally recovered from extra-oral infections [53]. We also recovered well-known potential respiratory pathogens, including *Pseudomonas aeruginosa* (8/31 patients) and *Staphylococcus aureus* (5/31 patients). Many other potentially opportunistic respiratory pathogens were found as well, including *Citrobacter koseri* (5/31), *Morganella morganii* (4/31) and members of the *Enterobacter cloacae* complex (3/31) [54–56]. From 26/31 ETs at least one *Candida* spp. was recovered, which is not surprising as *Candida* spp. are commonly present in healthy individuals and are often (in up to 80% of cases) the cause of nosocomial fungal infections [57]. We also recovered three isolates (from patient 1 and 3) that are likely *Aspergillus* spp., but could not be verified with the BDAL (MSP-8468, Bruker Daltonik) and the LM-UGent in-house (MSP-2876) identification databases. Overall, the culture-dependent identification showed that many potential pathogens associated with lung infections could be recovered from biofilms formed on ETs used to mechanically ventilate COVID-19 patients. No patterns of co-occurring species were observed, although identification of such

**Table 1**  
Summary of culture-dependent identification.

	Identification	Number of ETs from which taxon was recovered (n = 31)
Pseudomonadales	<i>Pseudomonas aeruginosa</i>	8
	<i>Moraxella</i> spp.	2
Enterobacterales	<i>Klebsiella aerogenes</i>	8
	<i>Klebsiella variicola</i>	2
	<i>Klebsiella</i> spp.	1
	<i>Escherichia/Shigella</i> spp. <sup>a</sup>	7
	<i>Citrobacter koseri</i>	5
	<i>Morganella morganii</i>	4
	<i>Enterobacter cloacae</i> complex	3
	Enterobacteriaceae spp. <sup>b</sup>	3
	<i>Hafnia alvei</i>	1
Other	<i>Stenotrophomonas</i> spp.	3
	Proteobacteria	1
	<i>Neisseria bacilliformis</i> , <i>Neisseria</i> spp., <i>Eikelenella</i> spp., <i>Aureimonas</i> spp., <i>Paracoccus yeei</i>	
Caryophanales	<i>Staphylococcus epidermidis</i>	24
	<i>Staphylococcus aureus</i>	5
	<i>Staphylococcus hominis</i>	4
	<i>Staphylococcus haemolyticus</i> ,	1
	<i>Staphylococcus capitis</i>	
	<i>Staphylococcus</i> spp.	9
	<i>Bacillus cereus</i> complex, <i>Bacillus subtilis</i> complex	1
	Lactobacillales	10
	<i>Enterococcus faecalis</i>	1
	<i>Enterococcus faecium</i>	1
	<i>Enterococcus</i> spp.	3
	<i>Streptococcus pneumoniae</i> ,	1
	<i>Streptococcus anginosus</i> ,	
	<i>Streptococcus parasanguinis</i> ,	
	<i>Streptococcus salivaris</i> , <i>Streptococcus sanguinis</i> , <i>Streptococcus vestibularis</i>	
	<i>Streptococcus</i> spp.	11
	<i>Lactocaseibacillus rhamnosus</i> ,	1
	<i>Lactocaseibacillus paracasei</i>	
	<i>Lactocaseibacillus</i> spp.	2
	<i>Lactobacillus</i> spp.	1
Other Firmicutes	<i>Veillonella</i> spp.	2
	<i>Megasphaera</i> spp.	2
	<i>Peptoniphilus</i> spp.	1
Actinobacteria	<i>Schaalia</i> spp.	2
	<i>Kytococcus schroeteri</i> , <i>Micrococcus luteus</i> , <i>Corynebacterium</i> spp., <i>Alloscardovia omnicolens</i> ,	1
	<i>Bifidobacterium</i> spp., <i>Gardnerella vaginalis</i> , <i>Slackia exigua</i>	
Bacteroidetes	<i>Prevotella</i> spp.	2
	<i>Bacteroides fragilis</i>	1
Fungi	<i>Candida albicans</i>	22
	<i>Candida tropicalis</i>	3
	<i>Candida kefyr</i>	1
	<i>Candida parapsilosis</i>	1
	<i>Candida</i> spp.	11

<sup>a</sup> MALDI-TOF MS was unable to distinguish between *Escherichia* spp. and *Shigella* spp.

<sup>b</sup> MALDI-TOF MS was unable to distinguish between *Klebsiella oxytoca* and a number of *Raoultella* spp.

patterns would likely be difficult, considering the relatively small sample size.

### 3.2. Culture-independent identification of bacteria based on 16S rRNA gene sequencing

16S rRNA amplicon sequencing was performed for DNA extracted from ET biofilms recovered from all 31 patients (Fig. 2). Overall, DNA from a large variety of potential lung pathogens was detected, including *Pseudomonas* spp. (31/31 patients, up to 99% of reads), *Streptococcus* spp. (30/31 patients, up to 57% of reads), *Staphylococcus* spp. (30/31 patients, up to 89% of reads), *Mycoplasma* spp. (30/31 patients, up to

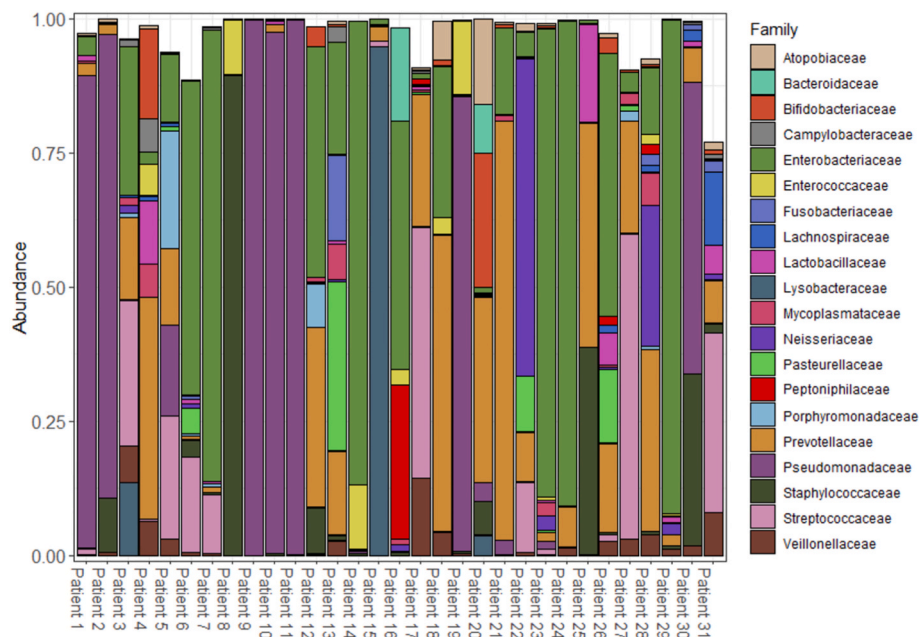


Fig. 2. Abundance of most-frequently identified bacterial families in every sample ('most-frequently identified' is defined as the top 20 across all the ET biofilms).

6.2% of reads), *Actinomyces* spp. (22/31 patients, up to 16% of reads), *Stenotrophomonas* spp. (18/31 patients, up to 94% of reads), *Haemophilus* spp. (17/31 patients, up to 14% of reads), *Klebsiella* spp. (16/31 patients, up to 78% of reads), *Enterobacter* spp. (12/31 patients, up to 92% of reads), *Morganella* spp. (8/31 patients, up to 1.2% of reads), and *Acinetobacter* spp. (12/31 patients, up to 0.1% of reads).

Using the culture-independent approach, taxa also identified with the culture dependent approach were generally found in relatively high abundances. Eight isolates recovered from six patients were not identified in these patients with the culture-independent approach, which could be due to their low relative abundance and/or sequencing depth. The isolates missing in the culture-independent approach belonged to the genera *Staphylococcus*, *Moraxella*, *Bacillus*, *Kytococcus*, *Aureimonas*, and *Paracoccus*. Nevertheless, compared to the culture-dependent approach, a large number of additional taxa per sample were detected with the culture-independent approach. Some taxa like *Fusobacterium* spp. (21/31 patients, up to 19% of reads) or *Rothia* spp. (7/31 patients, up to 2% of reads) were not found at all using culture-dependent approaches, while other taxa like *Neisseria* spp. (19/31 patients, up to 55% of reads), *Veillonella* spp. (25/31 patients, up to 8% of reads), and *Prevotella* spp. (30/31 patients, up to 77% of reads) were found to be more prevalent using the culture-independent approach. The differences between both approaches is most-likely due to the use of a limited set of selective and general media, that could have favored the recovery of certain abundant or fast-growing organisms, while more fastidious ones went undetected. In addition, recovery of strict anaerobes may have been hampered by the (extended) exposure to oxygen prior to and during sampling the ET.

Our data indicated that the bacterial diversity varied substantially between samples (Fig. 3A). Whereas the composition of some ET biofilms was diverse, other biofilms were dominated by a single pathogen. An example of such a dominant taxon is the genus *Pseudomonas*. DNA from *Pseudomonas* spp. was detected in all 31 patients and it made up a relatively large fraction (>50%) in seven of them, i.e. patients 1, 2, 9, 10, 11, 19 and 30. From these seven patients *Pseudomonas aeruginosa* was also isolated using the culture-dependent approach. It is known that *Pseudomonas aeruginosa* can inhibit the proliferation of other bacteria, leading to samples with low microbial diversity, which might also have occurred in these biofilms [58]. Indeed, a linear correlation between the decrease of the Simpson diversity index and the increase in *Pseudomonas*

abundance could be observed ( $R^2 = 0.59$ ,  $p < 0.001$ ; Fig. 3B), which would support this hypothesis. Of note, when we restrict this analysis to patients with a *Pseudomonas* abundance >1%, we get an even stronger linear correlation with an  $R^2$  of 0.92 ( $P < 0.001$ ) (Supplementary Fig. S1). ET biofilms recovered from several other patients were also dominated by a limited number of taxa. In patient 8 mainly sequences assigned to *Staphylococcus* spp. were found while in the biofilm from patient 15 mainly sequences from *Stenotrophomonas* spp. were found. Finally, ET biofilms recovered from patients 7, 14, 23, 24, and 29 were dominated by members of the *Enterobacteriales*. In patient 7, 83% of reads were identified as derived from *Escherichia* spp. or *Shigella* spp., in patient 23 68% of the reads were derived from *Klebsiella oxytoca* and 10% from another (unidentified) *Klebsiella* species, and in patient 29, 92% of reads were derived from *Enterobacter* spp. (likely a member of the *Enterobacter cloacae* complex based on the culture-dependent identification). For patient 14 and 24, the culture-independent approach did not allow identification to the species level, but based on the culture-dependent approach these sequences are likely derived from *Klebsiella aerogenes*. With the exception of the *Klebsiella* spp. in patient 23, these potential pathogens were also recovered in the culture-dependent approach, suggesting that both the culture-dependent and culture-independent methods are effective at finding the dominant pathogen.

### 3.3. Culture-independent identification of fungi based on ITS1 sequencing

ITS1 amplicon sequencing was done for 18 patients (for the remaining 13 patients not enough DNA could be recovered to perform ITS1 sequencing). The results of the ITS1 sequencing were similar for the different patients, with *Candida albicans* being detected in all 18 patients and making up >95% of the reads in 13/18 patients. Two of the other patients ET samples were dominated by *Candida dubliniensis* (patient 20: 94%; patient 7: 99% of reads) and two more by *Aspergillus* spp. (patient 1: 99% of reads; patient 28: 74%) (Fig. 4). From the ET biofilm of patient 1 (but not from patient 28) a putative *Aspergillus* spp. isolate was also identified using the culture-dependent approach. Besides *Aspergillus* spp. and *Candida* spp. only a few other fungal taxa were detected of which *Malassezia* spp. were the most common and most abundant (*Malassezia restricta* in 12/18 patients and up to 58% of reads, *Malassezia globosa* in 5/18 patients and up to 0.6% of reads, and *Malassezia sympodialis* in 2/

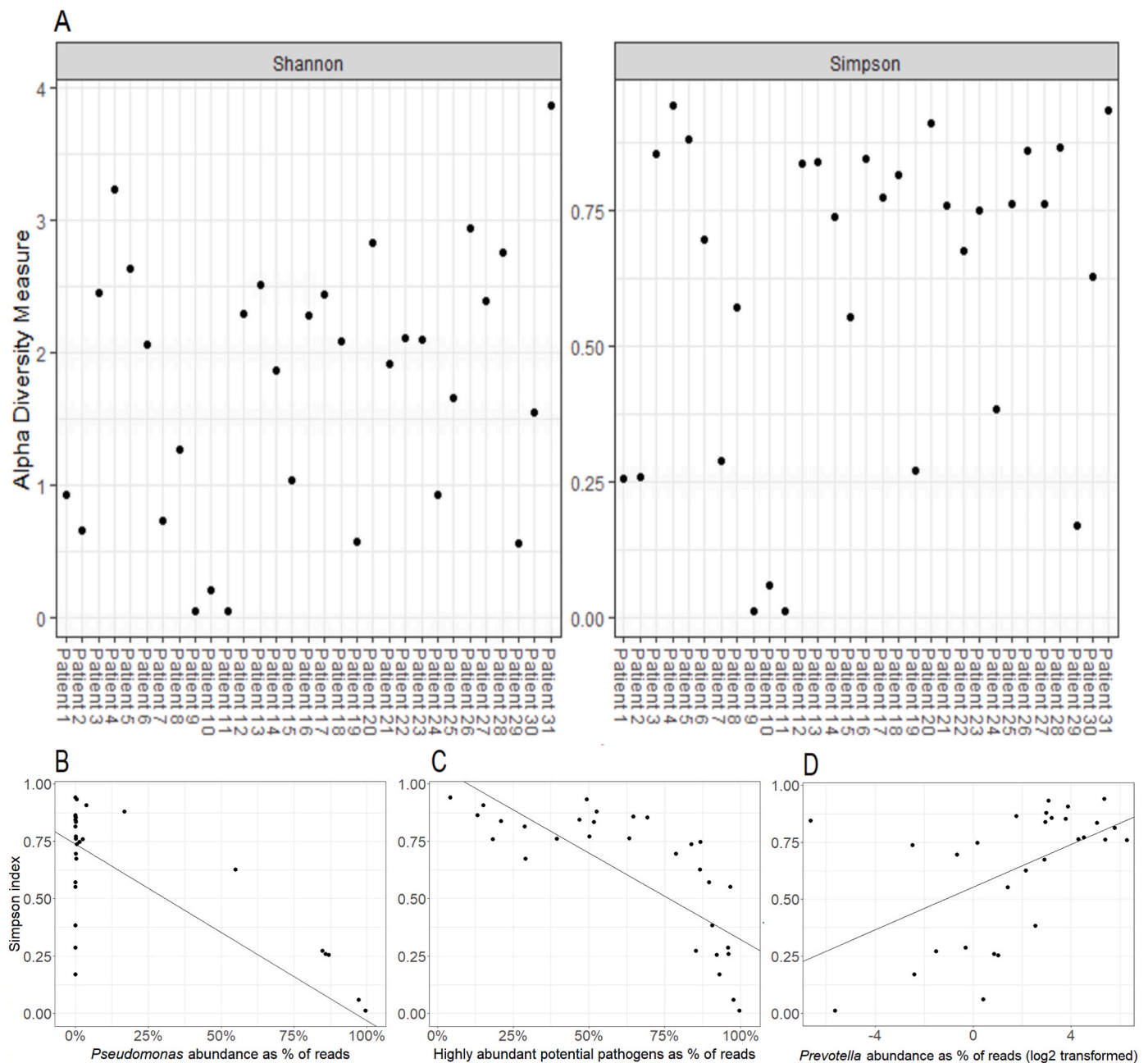


**Fig. 3.** A: Alpha diversity of ET biofilms based on their Shannon and Simpson index. B: Simpson index compared to abundance of *Pseudomonas* spp. as % of reads ( $R^2 = 0.59, p < 0.001$ ). C: Simpson index compared to combined abundance of the most abundantly identified potential pathogens (*Pseudomonas* spp., *Staphylococcus* spp., *Streptococcus* spp., *Stenotrophomonas* spp., members of the *Enterobacteriales*, *Haemophilus* spp., *Actinomyces* spp.) as % of reads (i.e. the sum of the relative abundances of each taxon) ( $R^2 = 0.57, p < 0.001$ ). D: Simpson index compared to abundance of *Prevotella* spp. as % of reads (log2 transformed) ( $R^2 = 0.28, p < 0.05$ ).

18 patients and up to 1.2% of reads). This predominance of *Candida* spp. is in line with what was observed using the culture-dependent identification approach.

### 3.4. Comparison with other (microbiome) studies

The composition of the lung microbiome can vary substantially between individuals depending on a multitude of factors, however *Bacteroidetes*, *Firmicutes*, and *Proteobacteria* have been most commonly isolated from healthy individuals [59]. Moving down to the genus level, *Prevotella*, *Streptococcus*, and *Veillonella* seem to be the most prevalent [60]. Potential pathogens are also frequently isolated from the respiratory tract of healthy individuals and include *Haemophilus* spp., *Neisseria* spp., and *Pseudomonas* spp.; these potential pathogens typically only

make up a small fraction of the community [59]. During an infection the lung microbiome is typically disturbed, and the prevalence of presumed commensals like *Prevotella* spp. decreases in favor of that of pathogenic bacteria [59–61]. On the ETs investigated in the present study common members of the lung microbiome were indeed found, with *Prevotella* spp., *Streptococcus* spp., and *Veillonella* spp. being identified in the majority of samples. However, in a considerable number of ETs, potential pathogenic bacteria dominated the biofilm, creating a community that seems more similar to that found during an infection in the lungs [62, 63]. A higher combined fraction of potential pathogens (*Pseudomonas* spp., *Staphylococcus* spp., *Streptococcus* spp., *Stenotrophomonas* spp., members of the *Enterobacteriales*, *Haemophilus* spp., and *Actinomyces* spp.) was correlated ( $R^2 = 0.57, p < 0.001$ ) with a lower Simpson diversity index (Fig. 3C). A modest correlation ( $R^2 = 0.28, p < 0.05$ )

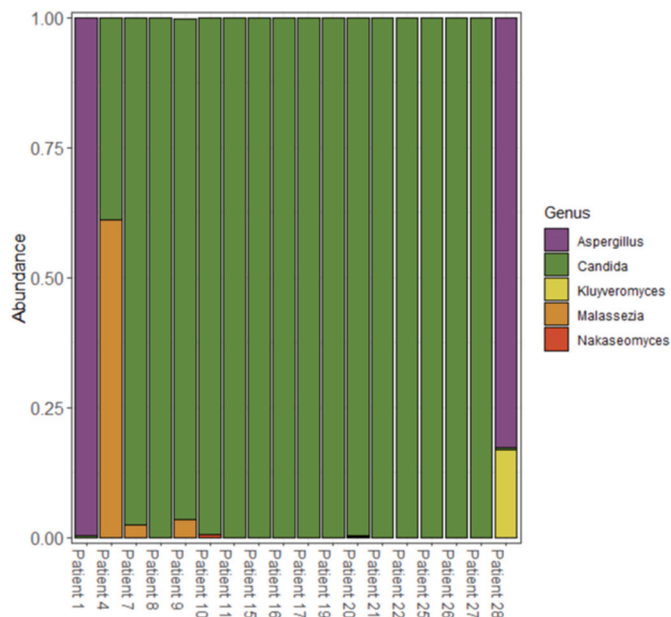


**Fig. 4.** Abundance of most-frequently identified fungal genera in every sample ('most-frequently identified' is defined as the top 5 across all the ET biofilms investigated).

between an increased abundance of *Prevotella* spp. and a higher Simpson diversity index was also observed (Fig. 3D).

Bacterial infections, both community or hospital acquired, have been reported with many respiratory viral infections. In influenza (the most studied viral infection in this context), infections with *Streptococcus pneumoniae*, *Staphylococcus aureus*, and *Haemophilus influenzae* are commonly reported, and these infections can severely affect disease outcome [64–66]. Infections with other potential pathogens like *Klebsiella* spp. and *Pseudomonas aeruginosa* have also been reported [67]. For COVID-19, hospital acquired infections are common with *Mycoplasma pneumoniae*, *Pseudomonas aeruginosa*, and *Haemophilus influenzae* [11]. Other pathogens found in the present study have also been reported, including *Enterobacter cloacae*, *Acinetobacter baumannii*, and *Klebsiella pneumoniae* [68]. These bacterial infections are all caused by species also identified in the ET biofilms investigated in the present study. Although the presence of these bacteria in the lungs does not seem to increase mortality in COVID-19 patients, they could be associated with potential severe complications and may extend the hospital stay of the patients [13,19]. Both the culture-dependent and culture-independent approach revealed that many potential lung pathogens were present in the ET biofilms. Combined, our data show that biofilms recovered from ETs from mechanically ventilated COVID-19 patients are diverse and contain many different organisms that are known to be clinically relevant. Although the small sample size and the diverse nature of the patient population investigated does not allow to link ET biofilm composition and clinical outcome, it is not unlikely that the ET biofilm may serve as a reservoir for subsequent lung infections.



**Fig. 5.** Prevalence of resistant (R), intermediate-resistant (I) and susceptible (S) bacterial isolates against aztreonam (AZT), ceftazidime (CAZ), clindamycin (CDM), gentamicin (GEN), meropenem (MEM), moxifloxacin (MXF), and vancomycin (VAN) for A: All tested isolates, B: *Klebsiella* spp., C: *Enterobacter* spp., D: *Pseudomonas aeruginosa*, E: *Staphylococcus* spp., F: *Enterococcus* spp.

### 3.5. Antimicrobial susceptibility

Resistance towards antibacterial agents varied between different antibiotics, i.e. from 0% (for vancomycin,  $n = 44$ ) to 68% (for meropenem,  $n = 123$ ) (Fig. 5A). The occurrence of resistance also varied between different genera (Fig. 5B–H), e.g. 42% of all *Klebsiella* spp. isolates investigated were resistant ( $n = 33$ ) to meropenem while this was 94% for *Pseudomonas aeruginosa* ( $n = 32$ ). Similarly, moxifloxacin resistance was observed in only 27% of all *Enterobacter* spp. isolates investigated ( $n = 15$ ), while 91% of all *Klebsiella* spp. isolates investigated ( $n = 33$ ) were resistant to this antibiotic. Antimicrobial susceptibility was lowest in *Pseudomonas aeruginosa*, which is not a surprise as this organism is notoriously resistant to many antibiotics [69,70]. Overall, the frequency of antimicrobial resistance was high, which was expected as these were samples from an ICU setting, where antibiotic resistance occurrence is typically high [71]. Additionally, it is likely that these patients were treated with antibiotics prior to and during the mechanical ventilation, which could potentially also lead to a higher incidence of resistance in the ET biofilm.

Overall, the frequency of resistance to antifungals was rather low (5% for caspofungin, 33% for fluconazole and 28% for itraconazole) (Fig. 6). No breakpoints were available for nystatin, but for all isolates except two, the zone of inhibition ranged from 19 mm to 28 mm. The two exceptions were two *Candida albicans* isolates with no zone of inhibition. These same two isolates were also resistant to caspofungin. As most of the isolates available for testing were identified as *Candida albicans*, a comparison of resistance between the different species is difficult, although it was noted that the five *Candida tropicalis* isolates, recovered from three ET biofilms, were all resistant to fluconazole and itraconazole.

For both antibacterial and antifungal agents, differences between isolates from the same ET biofilm were observed and are summarized in Table 2. This heterogeneity was observed in 14 out of 31 ETs for at least one species and one antibiotic. However for most ETs, only 1–4 isolates of the same species were tested and the criteria for heterogeneity were quite strict ( $\geq 5$  mm difference in zone of inhibition or  $\geq$  factor 8 difference in MIC value in a single ET biofilm). Because of these reasons, it seems likely that additional heterogeneity would be detected if antimicrobial susceptibility would be determined for more isolates and/or with less strict criteria. The highest number of isolates from the same species in a single ET biofilm were 10 *Pseudomonas aeruginosa* isolates (patient 10). In this case a single isolate was classified as R for ceftazidime while the nine others were classified as I. It is clear that if only 1 in 10 isolates shows reduced susceptibility, this could easily be missed if only a few were available for testing. While the experimental setup was not

**Table 2**

Heterogeneity in antimicrobial susceptibility against aztreonam (AZT), ceftazidime (CAZ), clindamycin (CDM), fluconazole (FLU), gentamicin (GEN), itraconazole (ITR), meropenem (MEM), and moxifloxacin (MXF) in isolates recovered from the same ET and belonging to the same MALDI-TOF cluster. Heterogeneity is defined as presence of isolates with  $\geq 5$  mm difference in zone of inhibition or  $\geq$  factor 8 difference in MIC value in a single ET biofilm.

Species	Antimicrobial(s) (number of ETs in which heterogeneity in susceptibility towards this antibiotic was observed/total number of ETs from which this species was isolated)	Number of ETs in which heterogeneity in susceptibility to any antibiotic was observed/total number of ETs from which this species was isolated
<i>Staphylococcus epidermidis</i>	CDM (4/28), GEN (5/28)	7/28
<i>Pseudomonas aeruginosa</i>	AZT (1/8), CAZ (2/8), MEM (1/8)	3/8
<i>Klebsiella aerogenes</i>	AZT (2/7), CAZ (2/7), MEM (1/7), MXF (1/7)	2/7
<i>Klebsiella variicola</i>	AZT (1/2), CAZ (1/2), MEM (1/2), MXF (1/2)	1/2
<i>Citrobacter koseri</i>	CAZ (1/5)	1/5
<i>Morganella morganii</i>	AZT (1/4)	1/4
<i>Candida parapsilosis</i>	FLU (1/1), ITR (1/1)	1/1

designed to accurately determine the prevalence of this heterogeneity in ET biofilms, it is clearly present and likely quite common. Heterogeneity in antimicrobial susceptibility could have important ramifications for antimicrobial susceptibility testing in a clinical setting in terms of how many isolates should be tested to determine whether a treatment would be effective. This type of heterogeneity in samples obtained from a single patient has been reported and investigated before, especially for cystic fibrosis patients [72], but should also be further investigated in relation to VAP in future studies.

### 3.6. Limitations of the present study

There are a number of limitations of this study, the first being the small sample size. Secondly, as patient identity was blinded, no clinical characteristics could be collected, which prevents us from identifying potential confounding factors that could affect biofilm composition (including -but not limited to- age, smoking status, comorbidities and medication status). Finally, we have no information on whether lung infection was present prior to COVID-19 infection and/or being admitted to the ICU.

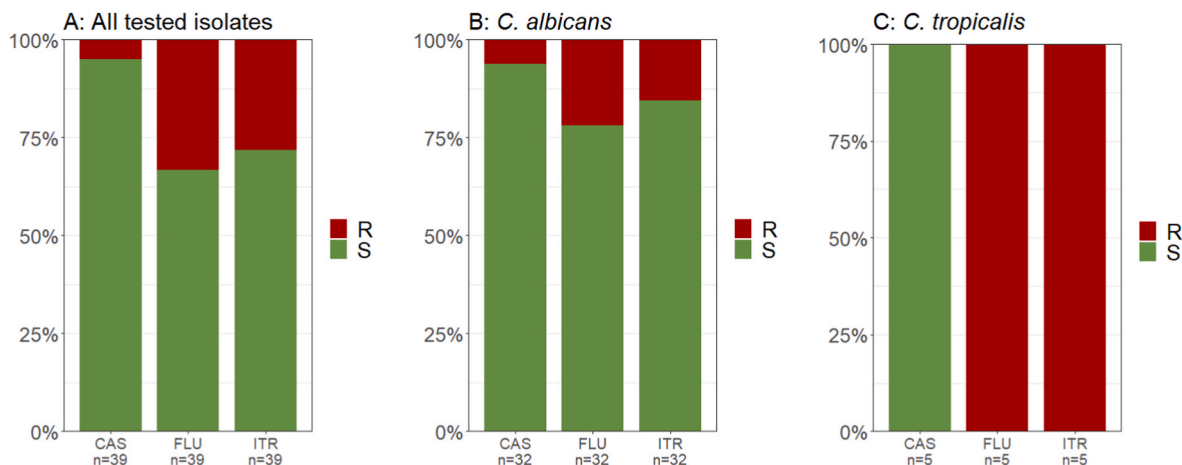


**Fig. 6.** Prevalence of resistant (R) and susceptible (S) *Candida* spp. isolates against caspofungin (CAS), fluconazole (FLU), and itraconazole (ITR) for A: All tested isolates, B: *Candida albicans*, and C: *Candida tropicalis*.



#### 4. Conclusion

Investigation of biofilms formed on 31 ETs obtained from mechanically-ventilated COVID-19 patients showed that these consisted of species that are typically part of the lung microbiome, and contained conventional respiratory pathogens. Where the culture-independent approach yielded a more complete picture of the biodiversity in these biofilms, the culture-dependent approach also allowed species level identification of the dominant potential pathogens. The taxa identified were similar to those observed in other studies investigating coinfections in COVID-19 patients and studies investigating coinfections that occurred with other respiratory viruses. Finally, results from the present study indicated that many isolates recovered from ET biofilms were resistant to commonly-used antibiotics, potentially further complicating treatment of infections in these patients.

#### CRedit authorship contribution statement

**Frits van Charante:** Investigation, Formal analysis, Writing – original draft. **Anneleen Wieme:** Writing – review & editing. **Petra Rigole:** Investigation. **Evelien De Canck:** Investigation. **Lisa Ostyn:** Investigation. **Lucia Grassi:** Investigation, Writing – review & editing. **Dieter Deforce:** Formal analysis, Supervision, Writing – review & editing. **Aurélien Crabbé:** Formal analysis, Supervision, Writing – review & editing. **Peter Vandamme:** Formal analysis, Supervision, Writing – review & editing. **Marie Joossens:** Formal analysis, Supervision, Writing – review & editing. **Filip Van Nieuwerburgh:** Investigation, Formal analysis, Supervision, Writing – review & editing. **Pieter Depuydt:** Resources, Writing – review & editing. **Tom Coenye:** Conceptualization, Investigation, Formal analysis, Supervision, Writing – original draft, Writing – review & editing, Project administration.

#### Declaration of competing interest

The authors declare the following financial interests/personal relationships which may be considered as potential competing interests: Frits van Charante reports financial support was provided by Special Research Fund Ghent University. Tom Coenye reports financial support was provided by the European Union Horizon 2020 Marie Skłodowska-Curie Actions program. Given his role as Senior Editor, Tom COENYE had no involvement in the peer review of this article and has no access to information regarding its peer review. Full responsibility for the editorial process for this article was delegated to Akos KOVACS.

#### Acknowledgements

We would like to thank the staff at the ICU of the Ghent University Hospital for making the extra effort to provide the ETs during the pandemic. F.v.C was funded through the European Union's Horizon 2020 research and innovation program under the Marie Skłodowska-Curie Grant Agreement No. 722467, (PrintAid project) and the Special Research Fund from Ghent University.

#### Appendix A. Supplementary data

Supplementary data to this article can be found online at <https://doi.org/10.1016/j.biofilm.2022.100079>.

#### References

- [1] Lv Z, Cheng S, Le J, Huang J, Feng L, Zhang B, et al. Clinical characteristics and coinfections of 354 hospitalized patients with COVID-19 in Wuhan, China: a retrospective cohort study. *Microb Infect* 2020;22(4–5):195–9. <https://doi.org/10.1016/j.micinf.2020.05.007>.
- [2] Alanio A, Delliere S, Fodil S, Bretagne S, Megarbane B. Prevalence of putative invasive pulmonary aspergillosis in critically ill patients with COVID-19. *Lancet Respir Med* 2020;8(6):e48–9. [https://doi.org/10.1016/S2213-2600\(20\)30237-X](https://doi.org/10.1016/S2213-2600(20)30237-X).
- [3] Dhesi Z, Enne VI, Brealey D, Livermore DM, High J, Russell C, et al. Organisms causing secondary pneumonias in COVID-19 patients at 5 UK ICUs as detected with the FilmArray test. *medRxiv* 2020;6(22):20131573. <https://doi.org/10.1101/2020.06.22.20131573>. 2020.
- [4] Zhu X, Ge Y, Wu T, Zhao K, Chen Y, Wu B, et al. Co-infection with respiratory pathogens among COVID-2019 cases. *Virus Res* 2020;285:198005. <https://doi.org/10.1016/j.virusres.2020.198005>.
- [5] De Bruyn A, Verellen S, Bruckers L, Geebelen L, Callebaut I, De Pauw I, et al. Secondary infection in COVID-19 critically ill patients: a retrospective single-center evaluation. *BMC Infect Dis* 2022;22(1):207. <https://doi.org/10.1186/s12879-022-07192-x>.
- [6] Adler H, Ball R, Fisher M, Mortimer K, Vardhan MS. Low rate of bacterial co-infection in patients with COVID-19. *The Lancet Microbe* 2020;1(2):e62. [https://doi.org/10.1016/S2666-5247\(20\)30036-7](https://doi.org/10.1016/S2666-5247(20)30036-7).
- [7] Bhatraju PK, Ghassemieh BJ, Nichols M, Kim R, Jerome KR, Nalla AK, et al. Covid-19 in critically ill patients in the seattle region - case series. *N Engl J Med* 2020;382(21):2012–22. <https://doi.org/10.1056/NEJMoa2004500>.
- [8] Schwab N, Nienhold R, Henkel M, Baschong A, Graber A, Frank A, et al. COVID-19 autopsies reveal underreporting of SARS-CoV-2 infection and scarcity of coinfections. *Front Med* 2022;9:868954. <https://doi.org/10.3389/fmed.2022.868954>.
- [9] Moreno-Garcia E, Puerta-Alcalde P, Letona L, Meira F, Duenas G, Chumbita M, et al. Bacterial co-infection at hospital admission in patients with COVID-19. *Int J Infect Dis* : *Int J Infect Dis* 2022;118:197–202. <https://doi.org/10.1016/j.ijid.2022.03.003>. official publication of the International Society for Infectious Diseases.
- [10] Langford BJ, So M, Raybardhan S, Leung V, Westwood D, MacFadden DR, et al. Bacterial co-infection and secondary infection in patients with COVID-19: a living rapid review and meta-analysis. *Clinic Microbiol Infect* 2020;26(12):1622–9. <https://doi.org/10.1016/j.cmi.2020.07.016>. the official publication of the European Society of Clinical Microbiology and Infectious Diseases.
- [11] Lansbury L, Lim B, Baskaran V, Lim WS. Co-infections in people with COVID-19: a systematic review and meta-analysis. *J Infect* 2020;81(2):266–75. <https://doi.org/10.1016/j.jinf.2020.05.046>.
- [12] Russell CD, Fairfield CJ, Drake TM, Turtle L, Seaton RA, Wootton DG, et al. Co-infections, secondary infections, and antimicrobial use in patients hospitalised with COVID-19 during the first pandemic wave from the ISARIC WHO CCP-UK study: a multicentre, prospective cohort study. *The Lancet Microbe* 2021;2(8):e354–65. [https://doi.org/10.1016/S2666-5247\(21\)00090-2](https://doi.org/10.1016/S2666-5247(21)00090-2).
- [13] Grasselli G, Scaravilli V, Mangioni D, Scudeller L, Alagna L, Bartoletti M, et al. Hospital-acquired infections in critically ill patients with COVID-19. *Chest* 2021; 160(2):454–65. <https://doi.org/10.1016/j.chest.2021.04.002>.
- [14] Sogaard KK, Baettig V, Osthoff M, Marsch S, Leuzinger K, Schweitzer M, et al. Community-acquired and hospital-acquired respiratory tract infection and bloodstream infection in patients hospitalized with COVID-19 pneumonia. *J Intensive Care* 2021;9(1):10. <https://doi.org/10.1186/s40560-021-00526-y>.
- [15] Bengoechea JA, Bamford CG. SARS-CoV-2, bacterial co-infections, and AMR: the deadly trio in COVID-19? *EMBO Mol Med* 2020;12(7):e12560. <https://doi.org/10.15252/emmm.202012560>.
- [16] Bosch AA, Biesbroek G, Trzcinski K, Sanders EA, Bogaert D. Viral and bacterial interactions in the upper respiratory tract. *PLoS Pathog* 2013;9(1):e1003057. <https://doi.org/10.1371/journal.ppat.1003057>.
- [17] Rice TW, Rubinson L, Uyeki TM, Vaughn FL, John BB, Miller 3rd RR, et al. Critical illness from 2009 pandemic influenza A virus and bacterial coinfection in the United States. *Crit Care Med* 2012;40(5):1487–98. <https://doi.org/10.1097/CCM.0b013e3182416f23>.
- [18] MacIntyre CR, Chughtai AA, Barnes M, Ridda I, Seale H, Toms R, et al. The role of pneumonia and secondary bacterial infection in fatal and serious outcomes of pandemic influenza a(H1N1)pdm09. *BMC Infect Dis* 2018;18(1):637. <https://doi.org/10.1186/s12879-018-3548-0>.
- [19] Sulaiman I, Chung M, Angel L, Tsay JJ, Wu BG, Yeung ST, et al. Microbial signatures in the lower airways of mechanically ventilated COVID-19 patients associated with poor clinical outcome. *Nat Microbiol* 2021;6(10):1245–58. <https://doi.org/10.1038/s41564-021-00961-5>.
- [20] Inglis TJ, Millar MR, Jones JG, Robinson DA. Tracheal tube biofilm as a source of bacterial colonization of the lung. *J Clin Microbiol* 1989;27(9):2014–8. <https://doi.org/10.1128/jcm.27.9.2014-2018.1989>.
- [21] Gibbs K, Holzman IR. Endotracheal tube: friend or foe? Bacteria, the endotracheal tube, and the impact of colonization and infection. *Semin Perinatol* 2012;36(6): 454–61. <https://doi.org/10.1053/j.semperi.2012.06.008>.
- [22] Perkins SD, Woeltje KF, Angenent LT. Endotracheal tube biofilm inoculation of oral flora and subsequent colonization of opportunistic pathogens. *Int J Med Microbiol : IJMM* 2010;300(7):503–11. <https://doi.org/10.1016/j.ijmm.2010.02.005>.
- [23] Danin PE, Girou E, Legrand P, Louis B, Fodil R, Christov C, et al. Description and microbiology of endotracheal tube biofilm in mechanically ventilated subjects. *Respir Care* 2015;60(1):21–9. <https://doi.org/10.4187/respcare.02722>.
- [24] Van Acker H, Van Dijk P, Coenye T. Molecular mechanisms of antimicrobial tolerance and resistance in bacterial and fungal biofilms. *Trends Microbiol* 2014;22(6):326–33. <https://doi.org/10.1016/j.tim.2014.02.001>.
- [25] Crabbe A, Jensen PO, Bjarnsholt T, Coenye T. Antimicrobial tolerance and metabolic adaptations in microbial biofilms. *Trends Microbiol* 2019;27(10): 850–63. <https://doi.org/10.1016/j.tim.2019.05.003>.
- [26] Adair CG, Gorman SP, Feron BM, Byers LM, Jones DS, Goldsmith CE, et al. Implications of endotracheal tube biofilm for ventilator-associated pneumonia. *Intensive Care Med* 1999;25(10):1072–6. <https://doi.org/10.1007/s001340051014>.

- [27] Vandecandelaere I, Matthijs N, Nelis HJ, Depuydt P, Coenye T. The presence of antibiotic-resistant nosocomial pathogens in endotracheal tube biofilms and corresponding surveillance cultures. *Pathogen Dis* 2013;69(2):142–8. <https://doi.org/10.1111/2049-632X.12100>.
- [28] Fernandez JF, Levine SM, Restrepo MI. Technologic advances in endotracheal tubes for prevention of ventilator-associated pneumonia. *Chest* 2012;142(1):231–8. <https://doi.org/10.1378/chest.11-2420>.
- [29] Kollef MH, Afessa B, Anzueto A, Veremakis C, Kerr KM, Margolis BD, et al. Silver-coated endotracheal tubes and incidence of ventilator-associated pneumonia: the NASCENT randomized trial. *JAMA* 2008;300(7):805–13. <https://doi.org/10.1001/jama.300.7.805>.
- [30] Rello J, Afessa B, Anzueto A, Arroliga AC, Olson ME, Restrepo MI, et al. Activity of a silver-coated endotracheal tube in preclinical models of ventilator-associated pneumonia and a study after extubation. *Crit Care Med* 2010;38(4):1135–40. <https://doi.org/10.1097/CCM.0b013e3181cd12b8>.
- [31] Thorarinsdottir HR, Kander T, Holmberg A, Petronis S, Klarin B. Biofilm formation on three different endotracheal tubes: a prospective clinical trial. *Crit Care* 2020;24(1):382. <https://doi.org/10.1186/s13054-020-03092-1>.
- [32] Rouze A, Martin-Loeches I, Nseir S. Airway devices in ventilator-associated pneumonia pathogenesis and prevention. *Clin Chest Med* 2018;39(4):775–83. <https://doi.org/10.1016/j.ccm.2018.08.001>.
- [33] Vandeplassche E, Coenye T, Crabbe A. Developing selective media for quantification of multispecies biofilms following antibiotic treatment. *PLoS One* 2017;12(11):e0187540. <https://doi.org/10.1371/journal.pone.0187540>.
- [34] Vanechoutte M, Verschraegen G, Claeys G, van den Abele AM. Selective medium for *Branhamella catarrhalis* with acetazolamide as a specific inhibitor of *Neisseria* spp. *J Clin Microbiol* 1988;26(12):2544–8. <https://doi.org/10.1128/jcm.26.12.2544-2548.1988>.
- [35] Kerr KG, Denton M, Todd N, Corps CM, Kumari P, Hawkey PM. A new selective differential medium for isolation of *Stenotrophomonas maltophilia*. *Eur J Clin Microbiol Infect Dis* 1996;15(7):607–10. <https://doi.org/10.1007/BF01709373>. official publication of the European Society of Clinical Microbiology.
- [36] Geary C, Stevens M. Rapid lysostaphin test to differentiate *Staphylococcus* and *Micrococcus* species. *J Clin Microbiol* 1986;23(6):1044–5. <https://doi.org/10.1128/jcm.23.6.1044-1045.1986>.
- [37] Church DL. Biochemical tests for the identification of aerobic bacteria. In: *Clinical microbiology procedures handbook*; 2016. 3.17.1.1–3.48.3.
- [38] Dumolin C, Aerts M, Verheyde B, Schellaert S, Vandamme T, Van der Jeugt F, et al. Introducing SPeDE: high-throughput dereplication and accurate determination of microbial diversity from matrix-assisted laser desorption-ionization time of flight mass spectrometry data. *mSystems* 2019;4(5). <https://doi.org/10.1128/mSystems.00437-19>.
- [39] Nelson MT, Pope CE, Marsh RL, Wolter DJ, Weiss EJ, Hager KR, et al. Human and extracellular DNA depletion for metagenomic analysis of complex clinical infection samples yields optimized viable microbiome profiles. *Cell Rep* 2019;26(8):2227–40. <https://doi.org/10.1016/j.celrep.2019.01.091>. e5.
- [40] Illumina. 2019. [https://support.illumina.com/content/dam/illumina-support/documents/documentation/chemistry\\_documentation/metagenomic/fungal-metagenomic-demonstrated-protocol-100000064940-01.pdf](https://support.illumina.com/content/dam/illumina-support/documents/documentation/chemistry_documentation/metagenomic/fungal-metagenomic-demonstrated-protocol-100000064940-01.pdf).
- [41] Illumina. 2013. [https://support.illumina.com/documents/documentation/chemistry\\_documentation/16s/16s-metagenomic-library-prep-guide-15044223-b.pdf](https://support.illumina.com/documents/documentation/chemistry_documentation/16s/16s-metagenomic-library-prep-guide-15044223-b.pdf).
- [42] Callahan BJ, McMurdie PJ, Rosen MJ, Han AW, Johnson AJ, Holmes SP. DADA2: high-resolution sample inference from Illumina amplicon data. *Nat Methods* 2016;13(7):581–3. <https://doi.org/10.1038/nmeth.3869>.
- [43] Martin M. Cutadapt removes adapter sequences from high-throughput sequencing reads. *EMBnetjournal* 2011;17(1). <https://doi.org/10.14806/ej.17.1.200>.
- [44] Quast C, Pruesse E, Yilmaz P, Gerken J, Schweer T, Yarza P, et al. The SILVA ribosomal RNA gene database project: improved data processing and web-based tools. *Nucleic Acids Res* 2013;41(Database issue):D590–6. <https://doi.org/10.1093/nar/gks1219>.
- [45] Nilsson RH, Larsson KH, Taylor AFS, Bengtsson-Palme J, Jeppesen TS, Schigel D, et al. The UNITE database for molecular identification of fungi: handling dark taxa and parallel taxonomic classifications. *Nucleic Acids Res* 2019;47(D1):D259–64. <https://doi.org/10.1093/nar/gky1022>.
- [46] McMurdie PJ, Holmes S. phyloseq: an R package for reproducible interactive analysis and graphics of microbiome census data. *PLoS One* 2013;8(4):e61217. <https://doi.org/10.1371/journal.pone.0061217>.
- [47] EUCAST. EUCAST disk diffusion method for antimicrobial susceptibility testing. In: *The European committee on antimicrobial susceptibility testing*; 2020. Version 8.0, 2020.
- [48] CLSI. Method for antifungal disk diffusion susceptibility testing of yeasts. third ed. Wayne, PA: Clinical and Laboratory Standards Institute; 2018. CLSI guideline M44.
- [49] EUCAST. Determination of minimum inhibitory concentrations (MICs) of antibacterial agents by broth dilution. *Clin Microbiol Infect* 2003;9(8):ix–xv. <https://doi.org/10.1046/j.1469-0691.2003.00790.x>.
- [50] EUCAST. Breakpoint tables for interpretation of MICs and zone diameters. In: *The European committee on antimicrobial susceptibility testing*; 2020. Version 10.0, 2020.
- [51] EUCAST. Breakpoint tables for interpretation of MICs for antifungal agents, version 10.0. In: *The European committee on antimicrobial susceptibility testing*; 2020.
- [52] CLSI. Performance standards for antifungal susceptibility testing of yeasts. second ed. Wayne, PA: Clinical and Laboratory Standards Institute; 2020. CLSI supplement M60.
- [53] Kawasuji H, Kaya H, Kawamura T, Ueno A, Miyajima Y, Tsuda T, et al. Bacteremia caused by *Slackia exigua*: a report of two cases and literature review. *J Infect Chemother* 2020;26(1):119–23. <https://doi.org/10.1016/j.jiac.2019.06.006>. official journal of the Japan Society of Chemotherapy.
- [54] Samonis G, Karageorgopoulos DE, Kofteridis DP, Matthaïou DK, Sidiropoulou V, Maraki S, et al. Citrobacter infections in a general hospital: characteristics and outcomes. *Eur J Clin Microbiol Infect Dis* 2009;28(1):61–8. <https://doi.org/10.1007/s10096-008-0598-z>. official publication of the European Society of Clinical Microbiology.
- [55] Liu H, Zhu J, Hu Q, Rao X. *Morganella morganii*, a non-negligible opportunistic pathogen. *Int J Infect Dis* 2016;50:10–7. <https://doi.org/10.1016/j.ijid.2016.07.006>. official publication of the International Society for Infectious Diseases.
- [56] Annavajhala MK, Gomez-Simmonds A, Uhlemann AC. Multidrug-resistant *Enterobacter cloacae* complex emerging as a global, diversifying threat. *Front Microbiol* 2019;10:44. <https://doi.org/10.3389/fmicb.2019.00044>.
- [57] Pendleton KM, Huffnagle GB, Dickson RP. The significance of *Candida* in the human respiratory tract: our evolving understanding. *Pathogen Dis* 2017;75(3). <https://doi.org/10.1093/femspd/ftx029>.
- [58] Hotterbeekx A, Xavier BB, Bielen K, Lammens C, Moons P, Schepens T, et al. The endotracheal tube microbiome associated with *Pseudomonas aeruginosa* or *Staphylococcus epidermidis*. *Sci Rep* 2016;6:36507. <https://doi.org/10.1038/srep36507>.
- [59] Beck JM, Young VB, Huffnagle GB. The microbiome of the lung. *Transl Res : J Lab Clin Med* 2012;160(4):258–66. <https://doi.org/10.1016/j.trsl.2012.02.005>.
- [60] Moffatt MF, Cookson WO. The lung microbiome in health and disease. *Clin Med* 2017;17(6):525–9. <https://doi.org/10.7861/clinmedicine.17-6-525>.
- [61] O'Dwyer DN, Dickson RP, Moore BB. The lung microbiome, immunity, and the pathogenesis of chronic lung disease. *J Immunol* 2016;196(12):4839–47. <https://doi.org/10.4049/jimmunol.1600279>. Baltimore, Md : 1950.
- [62] Millares L, Ferrari R, Gallego M, Garcia-Nunez M, Perez-Brocá V, Espasa M, et al. Bronchial microbiome of severe COPD patients colonised by *Pseudomonas aeruginosa*. *Eur J Clin Microbiol Infect Dis* 2014;33(7):1101–11. <https://doi.org/10.1007/s10096-013-2044-0>. official publication of the European Society of Clinical Microbiology.
- [63] Yin Y, Hountras P, Wunderink RG. The microbiome in mechanically ventilated patients. *Curr Opin Infect Dis* 2017;30(2):208–13. <https://doi.org/10.1097/QCO.0000000000000352>.
- [64] McCullers JA. The co-pathogenesis of influenza viruses with bacteria in the lung. *Nat Rev Microbiol* 2014;12(4):252–62. <https://doi.org/10.1038/nrmicro3231>.
- [65] Zhou F, Li H, Gu L, Liu M, Xue CX, Cao B, et al. Risk factors for nosocomial infection among hospitalised severe influenza A(H1N1)pdm09 patients. *Respir Med* 2018;134:86–91. <https://doi.org/10.1016/j.rmed.2017.11.017>.
- [66] Centers for Disease C, Prevention. Bacterial coinfections in lung tissue specimens from fatal cases of 2009 pandemic influenza A (H1N1) - United States. *MMWR Morbidity Mortal Week Rep* 2009;58(38):1071–4. May-August 2009.
- [67] Gao HN, Lu HZ, Cao B, Du B, Shang H, Gan JH, et al. Clinical findings in 111 cases of influenza A (H7N9) virus infection. *N Engl J Med* 2013;368(24):2277–85. <https://doi.org/10.1056/NEJMoa1305584>.
- [68] Mirzaei R, Goodarzi P, Asadi M, Soltani A, Aljanabi HAA, Jeda AS, et al. Bacterial co-infections with SARS-CoV-2. *IUBMB Life* 2020;72(10):2097–111. <https://doi.org/10.1002/iub.2356>.
- [69] Livermore DM. Multiple mechanisms of antimicrobial resistance in *Pseudomonas aeruginosa*: our worst nightmare? *Clin Infect Dis* 2002;34(5):634–40. <https://doi.org/10.1086/338782>. an official publication of the Infectious Diseases Society of America.
- [70] Botelho J, Grosso F, Peixe L. Antibiotic resistance in *Pseudomonas aeruginosa* - mechanisms, epidemiology and evolution. *Drug Resist Updates* 2019;44:100640. <https://doi.org/10.1016/j.drug.2019.07.002>.
- [71] Fridkin SK. Increasing prevalence of antimicrobial resistance in intensive care units. *Crit Care Med* 2001;29(4 Suppl):N64–8. <https://doi.org/10.1097/00003246-200104001-00002>.
- [72] Chung JC, Becq J, Fraser L, Schulz-Trieblaff O, Bond NJ, Foweraker J, et al. Genomic variation among contemporary *Pseudomonas aeruginosa* isolates from chronically infected cystic fibrosis patients. *J Bacteriol* 2012;194(18):4857–66. <https://doi.org/10.1128/JB.01050-12>.